IOP Conf. Series: Materials Science and Engineering **440** (2018) 012003 doi:10.1088/1757-899X/440/1/012003

Synthesis and characterization of carbamate insecticideintercalated zinc layered hydroxide modified with sodium dodecyl sulphate

Z Muda[1], N Hashim[1, 2*], I M Isa[1, 2], N M Ali[1], S A Bakar[2, 3], M Mamat[4], M Z Hussein[5], N A Bakar[1] and W R W Mahamod[1]

[1]Department of Chemistry, Faculty of Science and Mathematics, Universiti Pendidikan Sultan Idris, 35900 Tanjong Malim, Perak, Malaysia.
[2]Nanotechnology Research Centre, Faculty of Science and Mathematics, Universiti Pendidikan Sultan Idris, 35900 Tanjong Malim, Perak, Malaysia.
[3]Department of Physics, Faculty of Science and Mathematics, Universiti Pendidikan Sultan Idris, 35900 Tanjong Malim, Perak, Malaysia.
[4]Pusat Pengajian Sains Asas, Universiti Malaysia Terengganu, 21030 Kuala Terengganu, Terengganu, Malaysia.
[5]Materials Synthesis and Characterization Laboratory, Institute of Advanced Technology, Universiti Putra Malaysia, 43400 Serdang, Selangor, Malaysia.

Corresponding author email: norhayati.hashim@fsmt.upsi.edu.my

Abstract. A novel organic-inorganic nanocomposite based on carbamate insecticide-zinc layered hydroxide modified with sodium dodecyl sulphate nanocomposite (ZLH-SDS-PRO) was synthesized through ion exchange method of propoxur with commercially available zinc nitrate at various concentrations. The intercalation of propoxur into the interlayer of zinc layered hydroxide modified sodium dodecyl sulphate (ZLH-SDS) was confirmed by PXRD analysis with the basal spacing of the pure phase nanocomposite at 33.1 Å. The propoxur anions suggested to be arranged in a bilayer form between the galleries of zinc layered hydroxide. The intercalation also supported by Fourier transforms infrared spectra (FTIR) that showing the resemblance spectra between the host and the resulting nanocomposite. The elemental analysis estimates the loading of propoxur anion in the nanocomposite to be 88.17 %. The surface area analysis revealed mesoporous-type material properties for both the host and resulting nanocomposite. The thermal study shows a significant improved thermal stability of the propoxur anion compared to its pure form. The effect of intercalation of propoxur on the morphology of the host, ZLH-SDS crystals was investigated by field emission scanning electron microscopy (FESEM).

1. Introduction

Propoxur (2-isopropoxyphenyl N-methylcarbamate), a carbamate insecticide widely used in pest control for other domestic animals, mosquitoes, bugs, ants, gypsy moths, and other agricultural pests [1,2]. It was introduced to the market in 1959 and has been widely used against turf, forestry, and household pests and fleas [3]. It has been reported to produce a number of adverse effects including neurotoxicity and adversely affect memory and induce oxidative stress on both acute and chronic exposure [4].

The products of nanochemistry are being been used to create new generations of technologies for curing environmental maladies and protecting public health [5]. Water pollution control, groundwater remediation, potable water treatment, and air quality control are being advanced through nanomaterialbased membrane technologies [6], adsorbents [7], and catalysts [8–11]. Nanomaterial are also inspiring new solutions for providing and using energy that are more environmentally neutral than conventional approaches.

The modern day trend has induced the development of nanocomposite primarily based on natural polymers and inorganic solid mainly clay minerals [12]. Nano clays and layered double hydroxides (LDH) are being developed in this regard [12,13]. Both materials were reported to show excellent biocompatibility, low toxicity, and the potential for controlled release [14–18]. Various chemicals can be intercalated between layers of both materials such as 4-chloro-2-methylphenoxy acetic acid [15], polypropylene [18], 4-aminophenylsulfone [17], poly(methyl methacrylate) [19] and diclofenac [20].

Nowadays, another attention has been focused on zinc layered hydroxide (ZLH). Similarly, with LDH, ZLH structure is based on the mineral brucite ($Mg(OH)_2$) structure and categorised under layered hydroxide salt (LHS) [15]. Among the various two-dimensional layered materials, LHS have been of great interest due to their simple synthetic process and unique anion-exchange properties [21]. The structure of LHS is composed of positively charged hydroxide layers with charge-compensating anions in the interlayer spaces. Positive charges on layers are developed from under-coordination or mixed coordination geometries of interlayer cations. Therefore, counter-anions are required to stabilize the electrostatic charge of layers [22]. These modifications lead to a type of compounds called LHS, with the general formula $M^{2+}(OH)_{2-x}$ $(A^{m-})_{x/m}\cdot nH_2O$ where M^{2+} is the metal cation (e. g. Mg^{2+}, Ni^{2+} Zn^{2+},Ca^{2+},Cd^{2+},Co^{2+}, Cu^{2+}) and A^{m-} is the counter ion.

Occasionally, a few active agents are charged neutral and poorly-soluble pesticides which are difficult to be intercalate into the interlayer of ZLH. The majority of literatures are only focusing to the anionic pesticides. For charge-neutral and poorly water-soluble pesticides, their intercalation is usually dependent on anionic surfactant that forms a hydrophobic region in the gallery [23,24]. The hydrophobic nature and accessibility of the interlayer region of ZLH is helpful for adsorption of target pesticide molecules. In the previous study, Liu et al., [25] have developed a novel method to make chlorpyrifos (CPF) adsolubilize into the interlayer of zinc hydroxide nitrate (ZHN) intercalated with dodecylbenzenesulfonate (DBS). In this study, ZHN is modified with DBS to form a hydrophobic region in the gallery of ZHN−DBS. Liu et al., [25] suggests that DBS forms a tilt monolayer in the gallery when the SO_3 group approaches the layer by three oxygen atoms. The cationic and anionic surfactants interact to form neutral micelles, leaving the ZLH free to capture the desired anion. Since the interlayer spacing in the starting materials for this procedure is already quite large, this method offers particular promise for the incorporation of bulky anions [26].

Therefore, in this study, we discuss our work on the intercalation of propoxur, a carbamate insecticide, into the interlayer of ZLH modified with SDS by an ion exchange method, for the formation of a new organic-inorganic-layered nanocomposite material.

2. Method

2.1 Materials

Sodium dodecylsulphate (SDS) and zinc nitrate ($Zn(NO_3)_2\cdot 6H_2O$) were purchased from Systerm Malaysia. Sodium hydroxide, NaOH was purchased from HmbG Chemicals. Whereas, propoxur pesticide, $C_{11}H_{15}NO_3$ was purchase from Nanjing Essence Fine-Chemical. All solutions were prepared using deionized water. Each chemicals utilised in this synthesis were attained from several chemical providers and used without additional purification.

2.2 Synthesis of ZLH-SDS-PRO

The intercalation compound, ZLH-SDS-PRO was obtained via anion exchange between nitrate ion of precursor ZLH-SDS and anionic propoxur in a mixture solution of water: organic solvent. The host, layered zinc layered hydroxide-sodium dodecyl sulphate (ZLH-SDS) was synthesized by following

procedure describe elsewhere [25]. Briefly, ZLH-SDS was synthesized using co-precipitation method by the slow addition of 1.0 M NaOH and 40 mL of 0.5 M of $Zn(NO_3)_2 \cdot 6H_2O$, into a solution containing 40 mL of 0.25 M SDS under magnetic stirring. The pH value was adjusted to 6.5. The slurry was then centrifuged and dried in an oven at 70 °C.

Preparation of propoxur intercalated into the interlayer of ZLH-SDS (indicated as ZLH−SDS-PRO) was achieved by an ion exchange method. Various concentrations of propoxur solution were prepared at 0.0005 M, 0.0010 M, and 0.0025 M. 0.5 g of ZLH-SDS was dissociate in propoxur solution and keep under magnetic stirrer for 2 ½ hours. The slurry was then aged for 24 hours in an oil bath shaker at 70 °C. Then the slurry was centrifuged and the final white solid was dried in an oven for 24 hours.

2.3 Characterization

There are several instruments involved in the characterization of the ZLH-SDS-PRO nanocomposites. The X-ray powder diffraction patterns (PXRD) were obtained using a Power Diffraction Bruker AXS (model D8 Advance, wavelength of 1.5406 Å) with CuKα radiation at 60 kV and a current of 60 mA. The recorded region of 2θ was from 2° to 60° with a scanning rate of 2° min^{-1}. The FTIR spectra were collected in a Thermo Nicolet 6700 Fourier Transform Infrared Spectrometer in the range 400–4000 cm^{-1}. The thermal analyses measurement (TGA/DTG) of the sample was obtained with Perkin Elmer Pyris 1 TGA Thermo Balance with a heating rate of 20°C min^{-1} (N_2 flow rate is 50 ml/min, temperatures of 25-900 °C at a rate of 10 K/min). An inductive coupled plasma optical emission spectrometry (ICP-OES), model Agilent, 720 Axial and (CHNO-S), model Thermofinnigan, Flash EA 1112 was used to study the composition of the samples. The surface morphology of the sample was observed by a field emission scanning electron microscope (FESEM) Hitachi model SU 8020 UHR. Surface characterization of the nanocomposites was carried out by the nitrogen gas adsorption– desorption technique at 77 K using a Quantachrome Autosorb-1and degassed in an evacuated heated chamber at 120 °C overnight.

3. Results and discussion

3.1 PXRD analysis

Figure 1 shows the XRD pattern for the host, ZLH-SDS, propoxur anion and ZLH-SDS-PRO nanocomposite. The XRD pattern of ZLH-SDS showed a basal spacing of 9.8 Å corresponding to NO_3^-, and the peak at 33.0 Å has the same pattern with LDH-SDS that previously reported by [27]. The resulted ZLH-SDS is well crystallized without impurities like ZnO which indicated that a complete reaction during the co-precipitation between zinc nitrate and SDS. Upon dissolving zinc nitrate hexahydrate in water, the zinc species undergo hydrolysis reactions (Equation 1 and 2) as previously reported by Moezzi et al., [28].

$$Zn(NO_3)^2 \rightarrow Zn^{2+}(aq) + 2(NO_3)^-(aq) \quad (1)$$

$$Zn^{2+}(aq) + H_2O \rightleftharpoons ZnOH^+(aq) + H^+(aq) \quad (2)$$

Zinc hydroxide species can actually further transform into ZnO nanoparticles. However, in the presence of dodecyl sulphate ions, these zinc hydroxide species could cause charge–assemblies to form zinc hydroxide-dodecyl sulphate layered nanosheets. The formulas below (Equation 3 and 4) represent the main reactions that were previously reported by Liang et al. [29].

$$Zn(OH)_{2-x}^{x+} + x/4O_2 \rightarrow ZnO + (1 - 1/2x)H_2O \quad (3)$$

$$Zn(OH)_{2-x}^{x+} + xDS^- \rightarrow Zn(OH)_2 - xDS_x \quad (4)$$

The x-ray diffraction pattern of ZLH-SDS-PRO shows a series of basal peaks indicated by (003), (006), (009) in Figure 1. The intercalation of 0.0005M, 0.0010 M, and 0.0025 M, of propoxur pesticide into layered ZLH-SDS exhibited a diffraction pattern characterization with a sharp diffraction peak centred at 33.1 Å at low angle 2θ degree. By comparing the XRD pattern of the resulting with the pure propoxur, it can be observe that the resulting ZLH-SDS-PRO is in pure form without any impurities of

propoxur anion. This is due to due to successfully intercalation of propoxur between interlayer of ZLH-SDS well-ordered stacking layer. The sharp and intense intercalation peak reveal that the nanocomposite is high crystalinity [30]. The intensity of the intercalation peak of ZLHSDS-PRO nanocomposite decrease as the concentration of propoxur increases from 0.0010 to 0.0025 M indicates that the poorer crystalinity of nanocomposite at higher concentration of anion. This is due to the presence of the large amount of propoxur in interlayer and this is somehow interferes with the crystal growth during regeneration [31]. For further characterization, sample of 0.0010 M propoxur was then chosen as the phase pure well-ordered nanocomposite material and used for further characterizations.

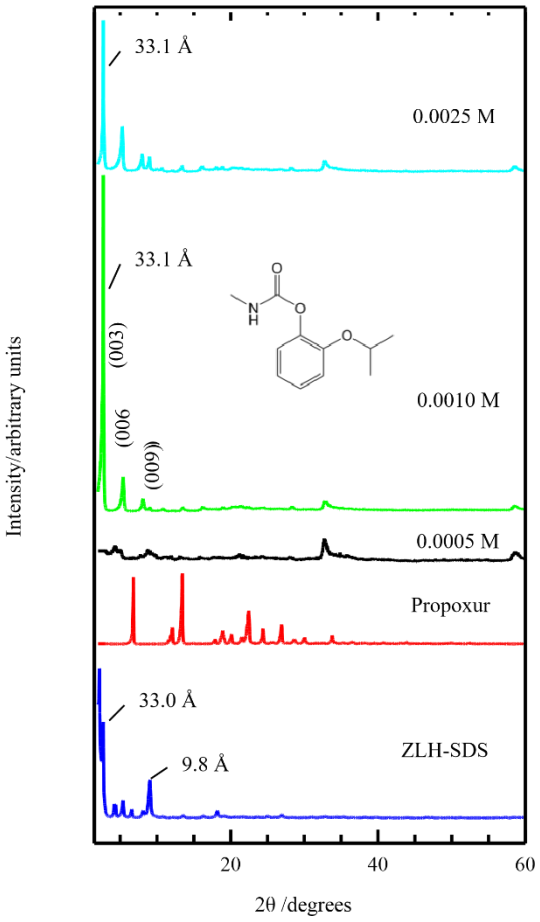

Figure 1. PXRD pattern for ZLH-SDS, propoxur anion, and ZLH-SDS-PRO nanocomposite with concentration of 0.0005 M, 0.0010 M and 0.0025 M of propoxur.

3.2 FTIR analysis

As shown in Figure 2, the propoxur spectra present adsorption peaks at 3309 cm^{-1} indicate the N-H for secondary amine group. The peaks appear at 1708 and 1253 cm^{-1} is due to stretching vibration of C=O and C-N group respectively. The C-O stretching vibration appears at 1197 and 1114 cm^{-1}. The C-H bending vibration peak appear at 1375 and 742 cm^{-1} while, C-H stretching vibration appear at 2963 cm^{-1}. Whereas, peak at 1496 cm^{-1} corresponds to the C-H stretching vibration for aromatic group. The list of FTIR peaks are presented in Table 1.

The FTIR spectra of ZLH-SDS shows a strong and sharp absorption band around 3500–3700 cm^{-1} corresponds to the stretching vibrations of the OH group of the free water molecule [32]. Whereas, a strong and broad absorption band centred at 3461 cm^{-1} attribute to the OH vibration. This band has a broad base due to hydrogen bonds established with the hydration water molecule [33]. Another bending vibration at 1637 cm^{-1} is the H-O-H bending of water molecule in the interlayer of ZLH-SDS. Two main doublet absorption bands appear in the region of 2850-2950 cm^{-1} which is due to stretching vibration of aliphatic group and another band at 1350-1480 cm^{-1} is due to bending vibration of aliphatic group.

While, the stretching vibration at 1210-1240 cm^{-1} is due to the presence of sulphate group in SDS (Hussein, Zainal, & Ming, 2000). A strong absorption band at 1364 cm^{-1} is due to the presence of nitrate as the salt used for the source of metal ions is zinc nitrate.

The FTIR spectra of ZLH-SDS-PRO nanocomposite resemble the ZLH-SDS spectra. A medium and broad band at 3507 cm^{-1} is attributing to the stretching vibration of the hydroxyl group of the water molecule in the interlayer. While, a peak at 1635 cm^{-1} reveal that there is a free water molecule in the interlayer of nanocomposite. A sharp doublet absorption of ZLH-SDS-PRO nanocomposite band resemble the peak in ZLH-SDS layer at 2913 and 2846 cm^{-1} which is due to stretching vibration of the C-H group that present in the nanocomposite. Whereas, the peak at 1375 and 742 cm^{-1} which is also resembles the peak in propoxur, is due to bending vibration of the aliphatic group, C-H. The bands appeared at 1202 and 1082 cm^{-1} is assigned to the asymmetric and symmetric stretching vibration of S=O [27]. The stretching vibration of S=O for ZLH-SDS-PRO particles are shifted to lower frequencies, indicating the configuration variation of the OSO_3^- functional group [27]. Those down-shift conforms to the losing of S=O bond strength, referring the existence of a hydrogen bond within ZLH interlayer and sulphate group (S=O H–O–Zn) as well as the electrostatic attraction [27]. The absence of N-H absorption peak in resulting ZLH-SDS-PRO spectra that should appear around 3350-3310 cm^{-1} indicating that propoxur molecule has been successfully loaded into the ZLH interlayer in an ion form. After the intercalation, propoxur maybe undergo elimination mechanism in hydrolysis reaction [35]. The intercalation also confirm by the disappearance of nitrate absorption peak which indicate the successful of ion exchange between nitrate ion and propoxur anion.

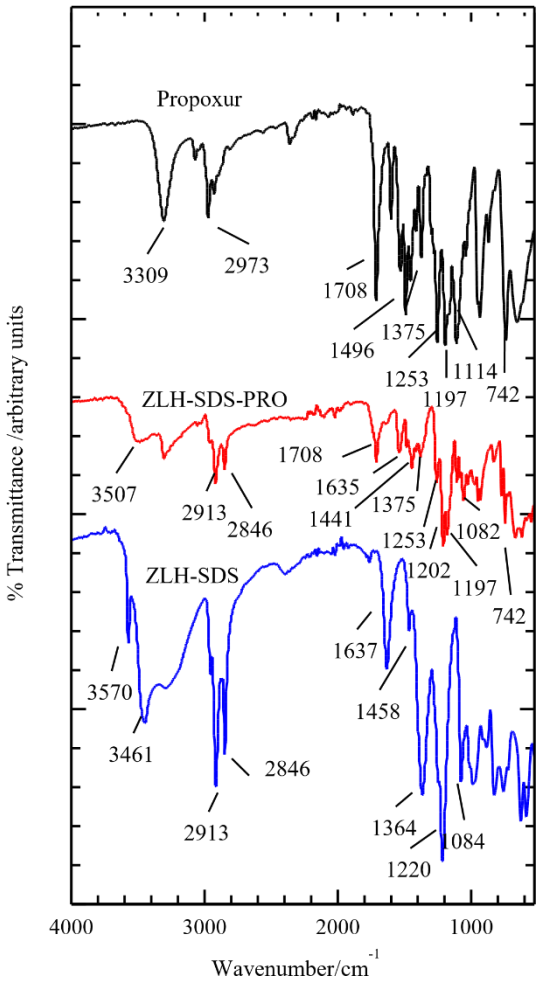

Figure 2. The FTIR spectra for ZLH-SDS, propoxur anion, and ZLH-SDS-PRO nanocomposite

Table 1. FTIR bands for ZLH-SDS, propoxur anion, and ZLH-SDS-PRO nanocomposite

Characteristic group	SDS	ZLH-SDS-PRO	Propoxur
ν (O-H), H-bonded	3461	-	-
ν (O-H) in the interlayer; H_2O	3570	3507	-
ν (H-O-H) in the interlayer; H_2O	1637	1635	-
ν (N-H)	-	-	3309
ν (C = O)	-	1708	1708
ν (C-O)	-	1197	1197
			1114
ν (C-N)	-	1253	1253
ν (C-H),stretching	2846	2846	2973
	2913	2913	
ν (C-H),bending	1458	1375	1375
		742	742
ν (C = C),stretching, aromatic	-	1441	1496
ν (N-O)	1364	-	-
	1637		
νas (S=O)	1220	1202	-
ν_s (S=O)	1084	1082	-

3.3 Spatial orientation

A proposed orientation of ZLH-SDS-PRO nanocomposite is shown in Figure 3. SDS and propoxur are aligned 90° perpendicular to the ZLH planes. Considering that propoxur anions and dodecyl sulphate ion electrostatically attracted to ZLH plane, the arrangement of the intercalated propoxur is proposed in bilayer arrangement as shown in Figure 3 (obtained by ChemDraw software). The interlayer height of ZLH-SDS-PRO nanocomposite is estimated by the basal spacing obtained from PXRD analysis which is 33.1 Å. Regarding the size of the propoxur molecule and interlayer space height of ZLHSDS-PRO nanocomposite, it is reasonable to conclude that the propoxur molecules are intercalated into the hydrophobic region formed by dodecyl sulphate molecules in the interlayer space of ZLH, due to the increase of the ZLH-SDS-PRO nanocomposite basal spacing, as reported elsewhere [27]. Since the layer thickness is 4.8 Å and the Zn^{2+} moiety of the lattice from the basal spacing is 2.6 Å, the interlayer height of the nanocomposite is estimated to be 23.1 Å.

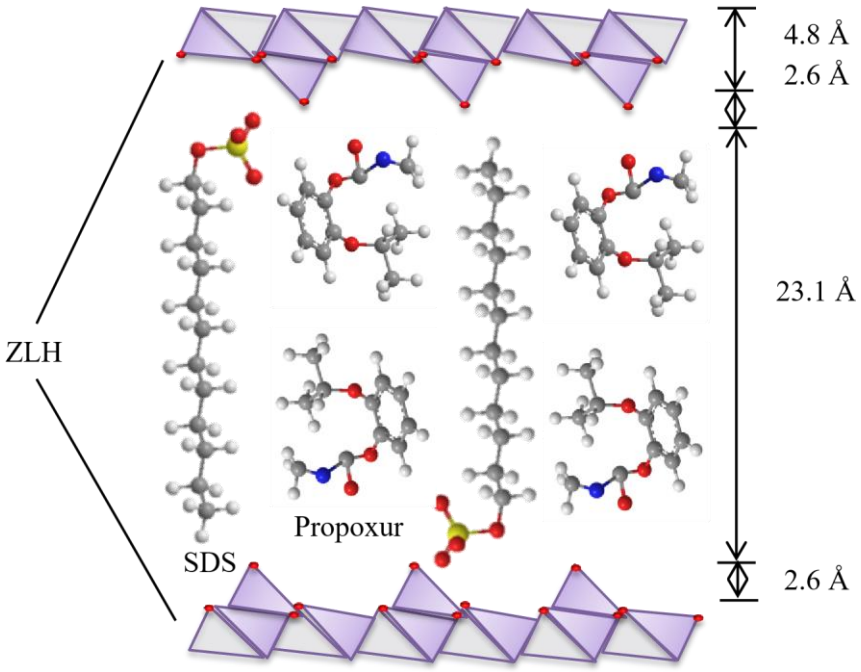

Figure 3. The proposed orientation of propoxur and SDS anions intercalated within the ZLH interlayer gallery resulting in ZLH-SDS-PRO nanocomposite estimated by Chemoffice software.

3.4 Elemental analysis

Elemental and compositional analysis of ZLH-SDS and ZLH-SDS-PRO nanocomposite are listed in Table 1. CHNO-S analysis of ZLH-SDS shows that 2.46 % of N, 24.8 % of C, 5.48 % of H, and 3.38 % of S. ICP-OES analysis shows high percentage of Zn (38.87 %) for pristine ZLH-SDS used in this work. After intercalation process, about 56.49 % of carbon is detected. The increase in percentage of C indicates successful intercalation of propoxur in the interlayer of ZLH [15]. The percentage of N in the resulting nanocomposites is 5.90 % and the percentage of S is 0.43 %. The S element represents the dodecyl sulphate ion in the interlayer of ZLH. The previously PXRD analysis confirmed that there was no nitrate ion after intercalation process. Therefore, the N element detected in the resulting nanocomposite came from the amine group in the propoxur anion, which also confirmed the successful intercalation of propoxur in the interlayer of ZLH. From CHNO-S data, the calculated percentage propoxur anion intercalates between the interlayer of ZLH region is 88.17 %. Whereas, the ICP-OES analysis detects 38.87 % of Zn in the resulting nanocomposite.

Table 2. Compositional data for synthesized ZLH-SDS and ZLH-SDS-PRO nanocomposite

Sample	N (%)	C (%)	H (%)	S (%)	Anion (% w/w)	% Zn
ZLH-SDS	2.46	24.80	5.48	3.38	-	24.14
ZLH-SDS-PRO	5.90	56.49	6.45	0.43	88.17	38.87

3.5 Thermal analysis

The thermogravimetric analysis, TGA-DTG obtained for propoxur, ZLH-SDS-PRO nanocomposite and ZLH-SDS are reported in Figure 4. In Figure 4 (a), the thermal study shows that the maximum temperature of pure propoxur was observed at 174 °C with 99.8 % of weight loss.

For ZLH-SDS-PRO nanocomposite, two stages of decomposition were observed in Figure 4 (b). The first stage is due decomposition of propoxur at 182 °C with weight loss of 63.5 %. Meanwhile the second stage is due to decomposition of SDS which can be observed at 218 °C with 4.2 % weight loss.

The ZLH−SDS display two stages of weight loss (Figure 4 (c)). The first stage corresponds to the removal of intercalated water at 107 °C with 3.2 % of weight loss [36]. Whereas, the decomposition of SDS takes place at 198 °C with a 37.0 % weight loss. From Figures 4(a) and (b), the maximum temperature of the decomposition of propoxur in the resulting nanocomposite increased from 174 °C to 182 °C. Therefore, the thermal study of ZLH-SDS-PRO nanocomposite affirm that the propoxur anion that intercalate in the ZLH-SDS interlayer is thermally stable compared to its prior form which is corresponding to the electrostatic interaction between anions and ZLH layer [37].

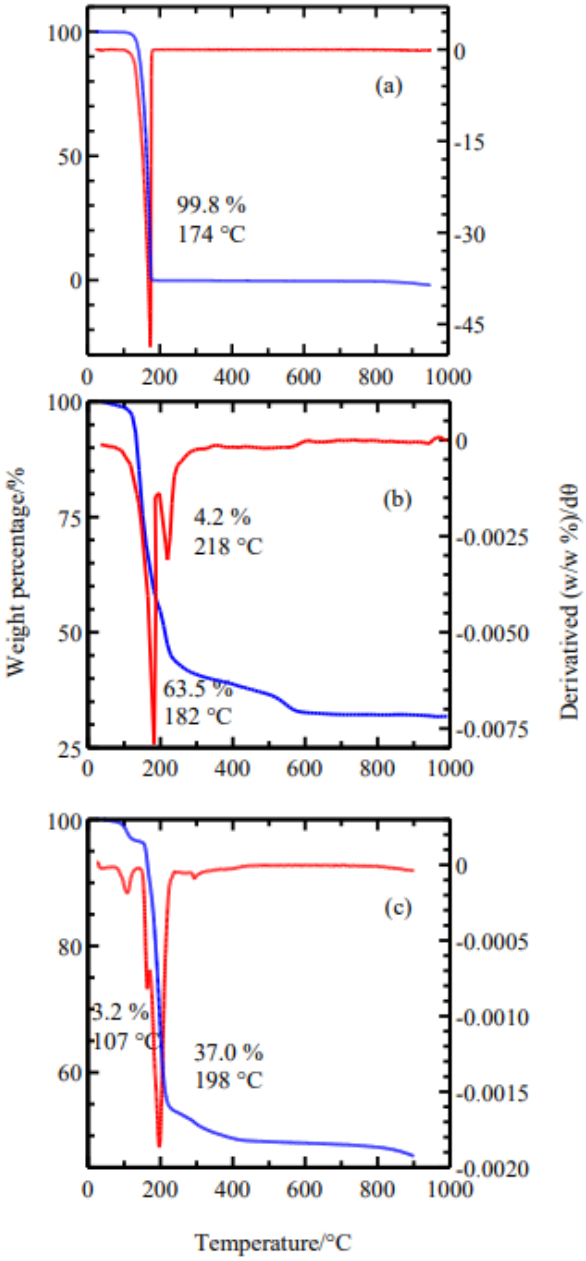

Figure 4. Termogravimetric curve for propoxur anion (a), ZLH-SDS-PRO nanocomposite (b), and ZLH-SDS (c).

3.6 Surface morphology analysis

Figures 5 (a) and 5 (b) illustrate the morphology of ZLH-SDS and ZLH-SDS-PRO at 10k magnification. The FESEM image of ZLH-SDS resemble thin flake-like nanosheets that are expected to be layered materials [38]. The edge of ZLH-SDS sheets is quite fractured with cracked surface. After the intercalation, 3D self-assemble nanoflower-like particle was observed with a size of a few microns. Miao et al., [21] has reported that, the nanoflower-like particle resulting from stirring in the intercalation process. The flower structure is composed of nanosheets which estimated to be 1.5-3.0 μm thickness of the nanosheets. The sheets are in stacked plate, sharp edges, and smooth surface.

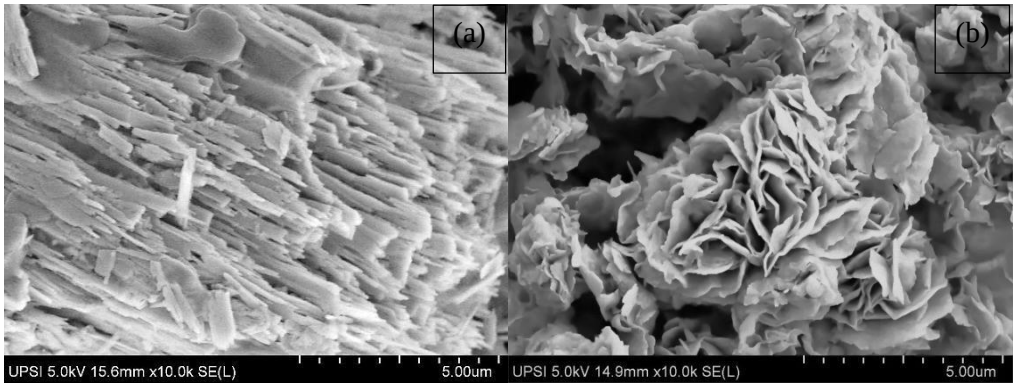

Figure 5. FESEM images of ZLH-SDS (a), and ZLH-SDS-PRO (b) 10k magnification nanocomposite

3.7 Surface area analysis

The comparison of surface area and porosity of ZLH-SDS and ZLH-SDS-PRO nanocomposite are given in Table 3. The intercalation of propoxur anion has decreased the BET surface area from 7.027 m^2g^{-1} for ZLH-SDS to 2.407 m^2g^{-1} for ZLH-SDS-PRO nanocomposite. This is attributed to the increase in the particles size and decrease of the pore volume [39].

As shown in Figure 6, both the host and resulted nanocomposites possessed a relatively narrow distribution of pores with an average diameter of 27.83 nm to 16.88 nm respectively, strongly suggesting the formation of a mesoporous structure. This is indicated by the closing of the pores from insertion of propoxur anion into the pores of the ZLH-SDS layer [20,40]. The nitrogen-adsorption isotherm for ZLH-SDS and ZLH-SDS-PRO nanocomposites are of Type IV isotherm with H3 hysteresis loops based on International Union of Pure and Applied Chemistry (IUPAC) classification [41] indicating mesopores-type materials [42]. The adsorption slowly increases in low relative pressure in the range of 0.0-0.6 (for ZLH-SDS) and 0.0-0.5 (for ZLH-SDS-PRO) which represents of the surface monolayer adsorption process. Further increases of the relative pressure resulting a rapid adsorption of the adsorbent due to the first multilayer adsorption. The presence of H3 hysteresis loop in layered ZLH-SDS and ZLH-SDS-PRO nanocomposite reveals that the pores exhibit slit-shaped pores with non-uniform shape and sizes. ZLH-SDS-PRO nanocomposite showed very much lower maximum adsorption compared to the host, ZLH-SDS which is due to the high capacity of propoxur anion intercalate in the interlayer of ZLH.

The Barret-Joyner-Halenda (BJH) pore size distribution for ZLH-SDS and ZLH-SDS-PRO nanocomposite is shown in Figure 7. The pore size distribution of ZLH-SDS and ZLH-SDS-PRO is almost the same features which centred at around 14 and 21 nm. In general, the pore size distributions do not show the formation of regular mesopores in the layered ZLH-nanocomposites, but could reveal the contribution of irregular mesoporous interparticulate void space [37,43].

Table 3. Surface properties of ZLH-SDS and ZLH-SDS-PRO nanocomposite

Samples	Specific BET surface area (m^2/g)	Average pore diameter (nm)	Classification
ZLH-SDS	7.027	27.83	Mesoporous
ZLH-SDS-PRO	2.407	16.88	Mesoporous

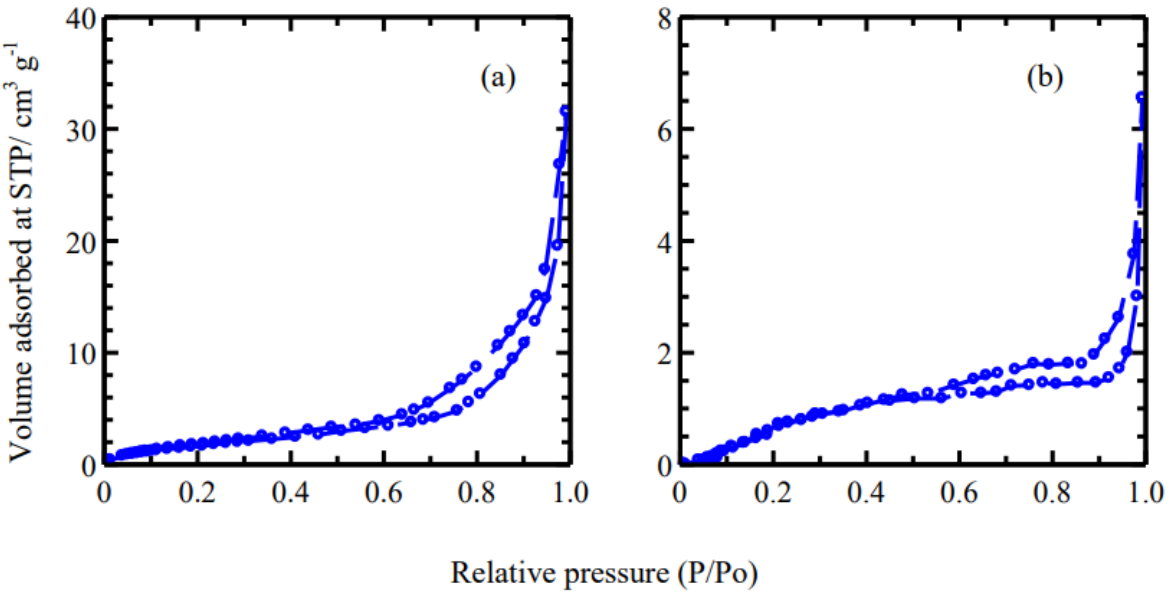

Figure 6. Adsorption–desorption isotherms of nitrogen gas for ZLH-SDS (a) and ZLH-SDS-PRO (b)

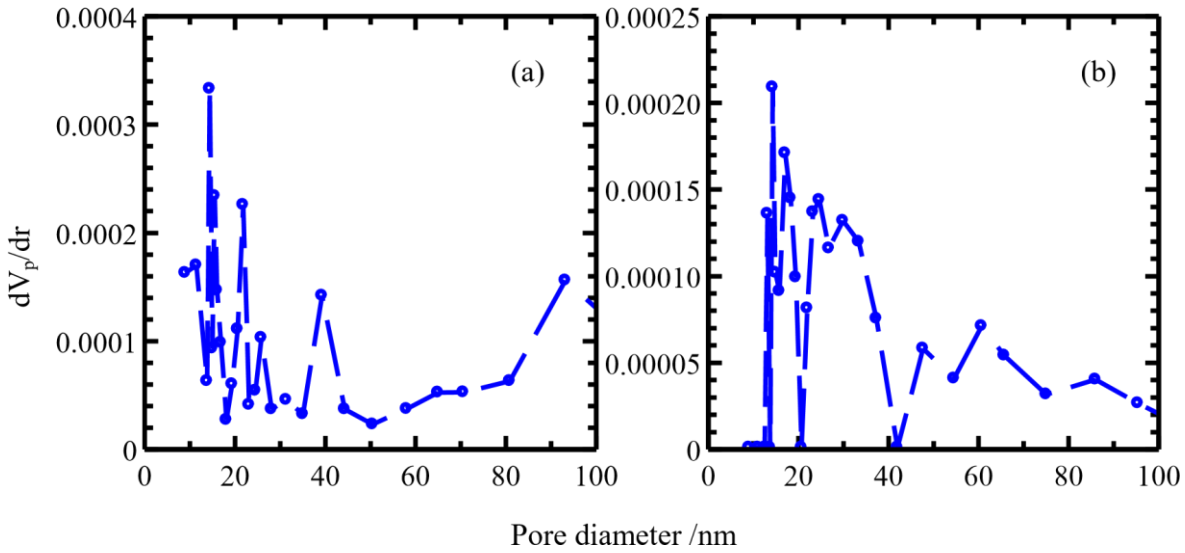

Figure 7. BJH desorption pore size distributions for ZLH-SDS (a), and ZLH-SDS-PRO (b)

4. Conclusion

In the present work, a carbamate insecticide, propoxur was successfully intercalated into the ZLH interlayer by ion exchange method. The modification of ZLH with SDS surfactant gives a great impact in order to intercalate the poor water soluble insecticide like propoxur into the interlayer of ZLH. A well-crystallized nanocomposite was obtained with basal spacing 33.1 Å. The FTIR spectra of ZLHSDS-PRO show a resemblance with ZLH-SDS spectra and propoxur spectra which support the intercalation of propoxur into interlayer of ZLH. The intercalation also has enhanced thermal stability of propoxur compared to its pure form. Both ZLH-SDS and the resulting nanocomposite show Type IV for the nitrogen adsorption–desorption isotherms with BET surface area 7.027 m^2g^{-1} and 2.407 m^2g^1, respectively. This nanocomposite also confirmed to exhibit mesoporous type material with remarkably flower-like surface morphology. The successful intercalation of propoxur proves that ZLH can be an excellent host for propoxur with SDS modification. Further work will be carried out with the controlled release formulation of this nanocomposite in order to study the release behaviour of this nanocomposite in selected medium.

5. References

[1] Pandey M R and Guo H 2014 Evaluation of cytotoxicity, genotoxicity and embryotoxicity of insecticide propoxur using flounder gill (FG) cells and zebrafish embryos *Toxicol. Vitr.* **28** 340–53

[2] Zafiropoulos A, Tsarouhas K, Tsitsimpikou C, Fragkiadaki P, Germanakis I, Tsardi M, Maravgakis G, Goutzourelas N, Vasilaki F, Kouretas D, Hayes A and Tsatsakis A 2014 Cardiotoxicity in rabbits after a low-level exposure to diazinon, propoxur, and chlorpyrifos. *Hum. Exp. Toxicol.* **33** 1241–52

[3] Tomlin C 1994 The pesticide manual; A world compendium, 10th edn. British Crop Protection Council

[4] Mehta K D, Garg G R, Mehta A K, Arora T, Sharma A K, Khanna N, Tripathi A K and Sharma K K 2010 Reversal of propoxur-induced impairment of memory and oxidative stress by 4′-chlorodiazepam in rats *Naunyn. Schmiedebergs. Arch. Pharmacol.* **381** 1–10

[5] Andrievski R A and Khatchoyan A V 2016 *Nanomaterials in Extreme Environments Fundamentals and Applications* (Switzerland: Springer Int. Publ)

[6] Pendergast M M and Hoek E M V 2011 A review of water treatment membrane nanotechnologies *Energy Environ. Sci.* **4** 1946–71

[7] M. Rozi Mat Dris, Chan Kok Sheng, M. Ikmar Nizam Isa M H R 2012 a Study of Cadmium Sulfide Nanoparticles With Starch As a *Int. J. Technol.* **1** 1–7

[8] Razali M H, Mohd Noor A F, Mohamed A R and Sreekantan S 2012 Morphological and structural studies of titanate and titania nanostructured materials obtained after heat treatments of hydrothermally produced layered titanate *J. Nanomater.* **2012**

[9] Razali M H, Ruslimie C A and Khairul W W 2013 Modification and performances of TiO2 photocatalyst towards degradation of paraquat dichloride *J. Sustain. Sci. Manag.* **8** 244–53

[10] Razali M H, Noor A F M and Yusoff M 2017 Hydrothermal synthesis and characterization of Cu^{2+}/F–Co-doped titanium dioxide (TiO_2) nanotubes as photocatalyst for methyl orange degradation *Sci. Adv. Mater.* **9** 1032–41

[11] Ahmad A, Razali M H, Mamat M, Mehamod F S B and Anuar Mat Amin K 2017 Adsorption of methyl orange by synthesized and functionalized-CNTs with 3-aminopropyltriethoxysilane loaded TiO_2 nanocomposites *Chemosphere* **168** 474–82

[12] Devi N and Maji T K 2011 Neem seed oil : Encapsulation and controlled release - search for a greener alternative for pest control *Pesticides in the Modern World-Pesticides Use and Management* pp 191–232

[13] Choy J H, Choi S J, Oh J M and Park T 2007 Clay minerals and layered double hydroxides for novel biological applications *Appl. Clay Sci.* **36** 122–32

[14] Dasgupta S 2017 Controlled release of ibuprofen using Mg Al LDH nano carrier *IOP Conf. Ser. Mater. Sci. Eng.* **225**
[15] Salleh N M, Mohsin S N, Sarijo S H and Ghazali S A I S M 2017 Synthesis and physicochemical properties of zinc layered hydroxide-4-chloro-2- methylphenoxy acetic acid (ZMCPA) nanocomposite *IOP Conf. Ser. Mater. Sci. Eng.* **204** 1–5
[16] Rehab A and Salahuddin N 2005 Nanocomposite materials based on polyurethane intercalated into montmorillonite clay *Mater. Sci. Eng. A* **399** 368–76
[17] Zulfiqar S, Ahmad Z, Ishaq M and Sarwar M I 2009 Aromatic-aliphatic polyamide/montmorillonite clay nanocomposite materials: Synthesis, nanostructure and properties *Mater. Sci. Eng. A* **525** 30–6
[18] Paiva L B de, Morales A R and Guimarães T R 2007 Structural and optical properties of polypropylene-montmorillonite nanocomposites *Mater. Sci. Eng. A* **447** 261–5
[19] Unnikrishnan L, Mohanty S, Nayak S K and Ali A 2011 Preparation and characterization of poly(methyl methacrylate)-clay nanocomposites via melt intercalation: Effect of organoclay on thermal, mechanical and flammability properties *Mater. Sci. Eng. A* **528** 3943–51
[20] Heraldy E, Suprihatin R W W and Pranoto 2016 Intercalation of diclofenac in modified Zn/Al hydrotalcite-like preparation *IOP Conf. Ser. Mater. Sci. Eng.* **107** 1–7
[21] Miao J, Xue M and Feng Q 2006 Hydrothermal synthesis of layered hydroxide zinc benzoate compounds and their exfoliation reactions 474–80
[22] Bae H S and Jung H 2012 Electron beam mediated simple synthetic route to preparing layered zinc hydroxide *Bull. Korean Chem. Soc.* **33** 1949–54
[23] Pavan P C, Crepaldi E L, De A. Gomes G and Valim J B 1999 Adsorption of sodium dodecylsulfate on a hydrotalcite-like compound. Effect of temperature, pH and ionic strength *Colloids Surfaces A Physicochem. Eng. Asp.* **154** 399–410
[24] Dekany I, Berger F, Imrik K and Lagaly G 1997 Hydrophobic layered double hydroxides (LDHs): Selective adsorbents for liquid mixtures *Colloid Polym. Sci.* **275** 681–8
[25] Liu J, Zhang X and Zhang Y 2015 Preparation and release behavior of chlorpyrifos adsolubilized into layered zinc hydroxide nitrate intercalated with dodecylbenzenesulfonate *ACS Appl. Mater. Interfaces* **7** 11180–8
[26] Auerbach S M, Carrado K a. and Dutta P K 2004 *Handbook of Layered Materials*
[27] Zhao J, Fu X, Zhang S and Hou W 2011 Water dispersible avermectin-layered double hydroxide nanocomposites modified with sodium dodecyl sulfate *Appl. Clay Sci.* **51** 460–6
[28] Moezzi A, Cortie M and McDonagh A M 2013 Formation of zinc hydroxide nitrate by H+catalyzed dissolution-precipitation *Eur. J. Inorg. Chem.* **2013** 1326–35
[29] Liang C, Tian Z, Tsuruoka T, Cai W and Koshizaki N 2011 Blue and green luminescence from layered zinc hydroxide/dodecyl sulfate hybrid nanosheets *J. Photochem. Photobiol. A Chem.* **224** 110–5
[30] Sarijo S H, Ghazali S A I S M, Hussein M Z and Sidek N J 2013 Synthesis of nanocomposite 2-methyl-4-chlorophenoxyacetic acid with layered double hydroxide: Physicochemical characterization and controlled release properties *J. Nanoparticle Res.* **15** 1536
[31] Costa F R, Leuteritz A, Wagenknecht U, Auf der Landwehr M, Jehnichen D, Haeussler L and Heinrich G 2009 Alkyl sulfonate modified LDH: Effect of alkyl chain length on intercalation behavior, particle morphology and thermal stability *Appl. Clay Sci.* **44** 7–14
[32] Yang W, Ma L, Song L and Hu Y 2013 Fabrication of thermoplastic polyester elastomer/layered zinc hydroxide nitrate nanocomposites with enhanced thermal, mechanical and combustion properties *Mater. Chem. Phys.* **141** 582–8
[33] Arizaga G G C, Gardolinski J E F D C, Schreiner W H and Wypych F 2009 Intercalation of an oxalatooxoniobate complex into layered double hydroxide and layered zinc hydroxide nitrate *J. Colloid Interface Sci.* **330** 352–8
[34] Hussein M Z, Zainal Z and Ming C Y 2000 Microwave-assisted synthesis of Zn-Al-layered double hydroxide-sodium dodecyl sulfate nanocomposite *J. Mater. Sci. Lett.* **19** 879–83

[35] Bakhti H and Hamida N Ben 2014 Kinetic study by uv spectrophotometry of isoprocarb degradation in aqueous medium *J. la Soc. Chim. Tunisie* **16** 35–43
[36] Nabipour H and Sadr M H 2015 Controlled release of diclofenac, an anti-inflammatory drug by nanocompositing with layered zinc hydroxide *J. Porous Mater.* **22** 447–54
[37] Hashim N, Muda Z, Isa I M, Ali N M, Bakar S A and Hussein M Z 2018 The effect of ion exchange and co-precipitation methods on the intercalation of 3-(4-methoxyphenyl)propionic acid into layered zinc hydroxide nitrate *J. Porous Mater.* **25** 249–58
[38] Liu J and Zhang Y 2016 Inorganic-organic nanohybrid materials of layered zinc hydroxide nitrate with intercalated salicylate: Preparation, characterization and Uv-blocking properties *Int. J. Nanosci.* **15** 1–9
[39] Hussein M Z, Al Ali S H, Zainal Z and Hakim M N 2011 Development of antiproliferative nanohybrid compound with controlled release property using ellagic acid as the active agent *Int. J. Nanomedicine* **6** 1373–83
[40] Hashim N, Hussein M Z, Yahaya A H and Zainal Z 2007 Formation of zinc aluminium layered double hydroxides-4-(2,4-dichlorophenoxy)butyrate nanocomposites by direct and indirect methods *Malaysian J. Anal. Sci.* **11** 1–7
[41] Sing K S W, Everett D H, Haul R a. W, Moscou L, Pierotti R a., Rouquérol J and Siemieniewska T 1985 Reporting physisorption data for gas/ solid system with special reference to the determination of surface area and porosity *Pure Appl. Chem.* **57** 603–19
[42] Wang J, Mei X, Huang L, Zheng Q, Qiao Y, Zang K, Mao S, Yang R, Zhang Z, Gao Y, Guo Z, Huang Z and Wang Q 2015 Synthesis of layered double hydroxides/graphene oxide nanocomposite as a novel high-temperature CO_2 adsorbent *J. Energy Chem.* **24** 127–37
[43] Hussein M Z, Ghotbi M Y, Yahaya A H and Abd Rahman M Z 2009 The effect of polymers onto the size of zinc layered hydroxide salt and its calcined product *Solid State Sci.* **11** 368–75

Acknowledgement
The author is grateful to the support for the research provided by UPSI under GPU Grant no. 20170188-101-01. ZM thanks UPSI for all funding and support for this research.